IOP Conference Series:
Earth and
Environmental Science

PURPOSE-LED PUBLISHING™

PAPER • **OPEN ACCESS**

Dynamic Modeling of Nitrogen Cycling in *Kappaphycus alvarezii* seaweed farming in Takalar, South Sulawesi

To cite this article: Jamaluddin Fitrah Alam *et al* 2026 *IOP Conf. Ser.: Earth Environ. Sci.* **1642** 012003

View the article online for updates and enhancements.

You may also like

- Design, Analysis, and Development of a Plastic Crusher for Recycling
Saad A. Mutasher, Mohammed Abdullah Alfazari, Anwar Hassan Sulieman Alkumzari et al.
- Integrating Local Wisdom into Sustainable Residential Design in Makassar
Reinny Devi F. Razak, Reza Yuniar Sandi, Hardiansyah et al.
- Effect of Pre-treatment of Oil Palm Empty Fruit Bunch (OPEFB) in the production of biogas in Chemical Looping Reforming (CLR)
Nuralia Rezwan, Nurfanizan Afandi, Abreeza Manap et al.

This content was downloaded from IP address 87.49.43.243 on 04/10/2026 at 16:48

IOP Conf. Series: Earth and Environmental Science **1642** (2026) 012003 doi:10.1088/1755-1315/1642/1/012003

Dynamic Modeling of Nitrogen Cycling in *Kappaphycus alvarezii* seaweed farming in Takalar, South Sulawesi

Jamaluddin Fitrah Alam[1,2*], Nita Rukminasari[2,3], Asmi Citra Malina[3], Amanda Pricella Putri[3], Andi Alya Yusriyyah[1], Nur Halizah Roebetho[3], Putri Sakinah Resman[3], Rahmat Pratama Putra[3]

[1] Department of Marine Science, Faculty of Marine Science and Fisheries, Hasanuddin University, Makassar, Indonesia
[2] Climate Change and Coastal Resilience Research Group, Hasanuddin University, Makassar, Indonesia
[3] Department of Fisheries, Faculty of Marine Science and Fisheries, Hasanuddin University, Makassar, Indonesia

[*]E-mail: alamjamaluddin@unhas.ac.id

Abstract. This study examines the nitrogen cycle within seaweed (*Kappaphycus alvarezii*) farming systems in the coastal waters of Takalar, South Sulawesi, utilizing a combination of field observations and dynamic systems modeling. Field data were employed to construct a system dynamics model using STELLA Architect 13.1. The observed data on nitrogen and seaweed biomass were used to validate the model. The model successfully replicated the observed pattern of low ammonium and high nitrate levels early in the cycle, which declined to a minimum mid-cycle and partially recovered before harvest; the associated biomass response exhibited rapid early growth, a mid-cycle slowdown, and a modest late increase. Reproducibility was notably high for nitrate (PBIAS −13.3%) and biomass (PBIAS +8.1%), while ammonium remained near detection limits and was assessed qualitatively. These findings suggest that nitrate regeneration and availability within the cycle are critical controls on farm-scale biomass accumulation and provide a validated framework for analyzing nitrogen effects on *K. alvarezii* production in this area.

1. Introduction

Coastal ecosystems represent dynamic environments influenced by both natural processes and anthropogenic activities. Alterations in nutrient cycling, primarily driven by agricultural runoff, domestic effluents, and aquaculture discharges, can disrupt the balance of dissolved nitrogen in nearshore waters. An excess of nitrogen frequently leads to eutrophication, which is characterized by rapid algal proliferation, reduced dissolved oxygen levels, and a decline in biodiversity. Conversely, nitrogen depletion can limit primary productivity and hinder the growth of marine primary producers (1–3). Therefore, a comprehensive understanding of nitrogen dynamics is crucial for maintaining ecological balance and supporting sustainable aquaculture in coastal zonesSee the separate guidelines document for further information.

Content from this work may be used under the terms of the Creative Commons Attribution 4.0 licence. Any further distribution of this work must maintain attribution to the author(s) and the title of the work, journal citation and DOI.
Published under licence by IOP Publishing Ltd

Seaweed farming provides an ecosystem-based pathway to mitigate nutrient disturbances. *Kappaphycus alvarezii* can assimilate dissolved inorganic nitrogen from the water column and thereby function as a natural biofilter while supporting coastal livelihoods (4). Indonesia, particularly South Sulawesi, is among the world's leading carrageenophyte producers; the sector delivers employment and income for coastal communities but remains sensitive to environmental variability (5,6). Sustained production depends on nutrient availability together with temperature, hydrodynamics, and dissolved oxygen, all of which fluctuate across sites and seasons (6).

Takalar, South Sulawesi, is a major center of *K. alvarezii* cultivation where farmers report strong links between within-cycle nitrogen supply, specific growth rate, and final biomass. Adequate nitrogen supports rapid thallus growth, whereas limitation is associated with reduced yields and elevated disease risk, including ice-ice (7,8). Yet the degree to which temporal fluctuations in nitrogen across a single cultivation cycle constrain growth and harvestable biomass at farm scale remains weakly quantified.

Nitrogen in farming areas arises from external inputs (e.g., land-based sources) and internal processes in the water column and sediments, including remineralization of organic matter. Uptake by seaweed is not constant; it varies with temperature, current velocity, and oxygen availability (6). At commercial scale, nitrogen variability during a harvest cycle can directly affect specific growth rate and biomass yield, underscoring the need to evaluate the nitrogen balance over a full cultivation cycle (2). However, direct high-frequency monitoring of nitrogen dynamics is challenging due to the complexity and coupling of processes.

Dynamic system modeling offers a tractable approach to integrate these processes and quantify how nitrogen cycling influences growth and productivity. Such models have advanced understanding in aquatic ecology and aquaculture by representing uptake, storage, and use of nutrients, and have been applied in several studies in related coastal systems (e.g., nutrient budgets around artificial timber reefs) (9,10). Here, we develop and validate a system-dynamics model of the nitrogen balance for a single cultivation cycle of *K. alvarezii* in Takalar. We integrate field observations of nitrogen types, seaweed biomass, and environmental drivers to (i) quantify how temporal nitrogen variability affects growth and yield and (ii) explore scenarios to maintain productivity under variable nutrient supply. The results aim to support evidence-based decisions for efficient and sustainable seaweed farming in Indonesian coastal waters.

2. Methods

The study covered a single 40-day cultivation cycle from 23 April to 25 May 2025 in coastal waters off Aeng Batu-Batu Village, North Galesong Subdistrict, Takalar Regency, South Sulawesi, Indonesia (5°14′10″ S, 119°22′53″ E). A 10 × 15 m plot of *Kappaphycus alvarezii* and the immediately surrounding waters were observed, with nearby non-farming waters used as an open-water control. Regional hydrography is shaped by semidiurnal tides and coastal circulation influenced by the Jeneberang River plume.

Weekly field observations were combined with a dynamic systems model to quantify nitrogen cycling and its effects on seaweed growth. On each visit five stations were sampled: three within the farm plot to capture within-farm variability and two in adjacent open waters outside the cultivation footprint. Sampling was conducted on Days 0, 8, 16, 24, 32, and 40, spanning one complete cultivation cycle.

At each station, near-surface seawater (≈30 cm depth) was collected into 500 mL acid-washed, dark HDPE bottles, stored in an insulated cool box, and transported to the laboratory for

analysis within 24 h. Subsamples (25–50 mL) were filtered for nutrient determinations using 0.45 µm membrane filters (Millipore) for ammonium (NH_4^+) and Whatman No. 42 ashless cellulose filters for nitrate (NO_3^-). Ammonium was measured spectrophotometrically by the phenate–nitroprusside method with absorbance at 640 nm; nitrate was determined colorimetrically via the brucine–H_2SO_4 method with absorbance at 410 nm on a benchtop spectrophotometer. Concentrations are reported as mg m^{-3}; internal checks used the conversion 1 mg L^{-1} = 1000 mg m^{-3} with laboratory calibration curves.

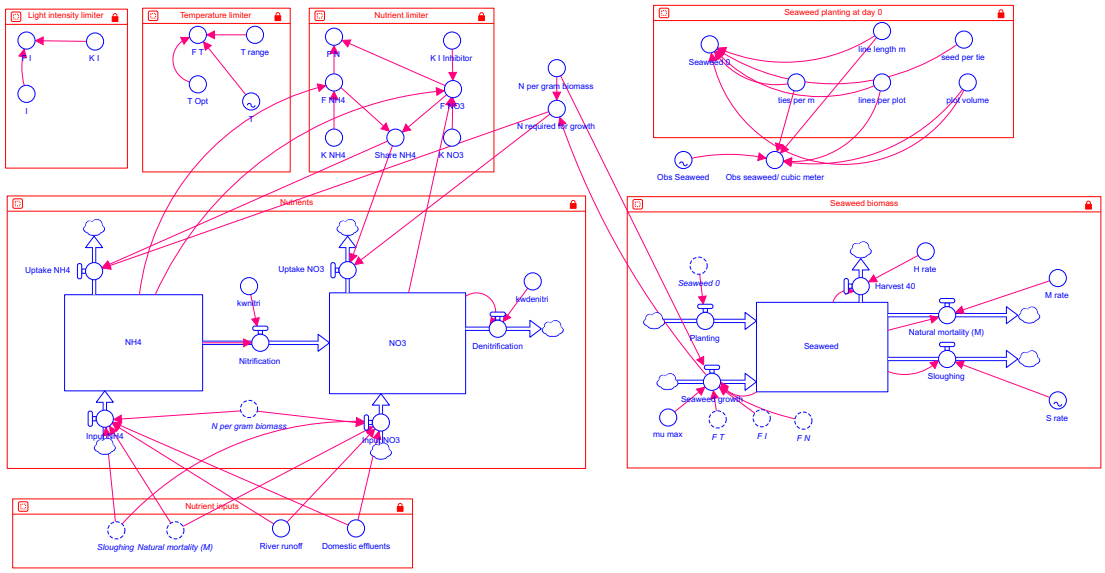


Figure 1. Stock–flow diagram of the nitrogen–biomass model. Modules: (A) light limiter; (B) temperature limiter; (C) nutrient limiter with NH_4^+ priority and NH_4^+ inhibition of NO_3^- uptake; (D) seeding/harvest pulses and plot geometry; (E) external nutrient inputs (domestic effluents, river runoff) and internal regeneration from sloughing and natural mortality; central nitrogen boxes for (F) NH_4^+ with nitrification to NO_3^- and (G) NO_3^- with denitrification; (H) seaweed biomass with growth and loss processes. Arrows show causality; double arrows indicate stock–flow connections.

In situ physicochemical variables comprised temperature (°C), pH, and dissolved oxygen (DO, mg L^{-1}) measured with a portable multiparameter meter (Toa DKK WQC-24), calibrated daily. Salinity (ppt) was recorded from the meter's conductivity probe. Near-surface current speed (m s^{-1}) was estimated with the floating method. All variables were measured on site during each weekly visit.

Within the 10 × 15 m plot, wet weight (WW) of *K. alvarezii* was recorded at Day 0 and at 7-day intervals using a field scale. Each week, 17 tagged samples (thalli/ties) were weighed to derive plot-level growth trends, and at harvest (≈Day 40) the full plot biomass was weighed to estimate total production.

The model resolves three coupled stocks—ammonium (NH_4^+), nitrate (NO_3^-), and seaweed biomass (g WW m^{-3})—linked by mass-balanced flows and driven by environmental limiters (light, temperature, nutrients) and management pulses (seeding and harvest).

The stock flow nitrogen enters from external sources (domestic effluents, river runoff) and from internal regeneration associated with biomass losses (natural mortality and sloughing). Within the water column, NH_4^+ is oxidized to NO_3^- by nitrification; NO_3^- is removed by denitrification. Seaweed takes up nitrogen from both substrates; the total uptake equals the

nitrogen required to support realized growth, so nitrogen withdrawn from the water column is exactly accounted for in biomass gain. Planting is represented as a pulse at Day 0 and harvest as a pulse at Day 40. All concentrations are in mg m^{-3} and biomass in g WW m^{-3}, with explicit plot-volume conversions. The mass balances follow the stock–flow structure and are written as ordinary differential equations. For ammonium (NH4) and nitrate (NO3):

$$\frac{d\,NH4}{dt} = External + Internal - Uptake_NH4 - k_nitri \cdot NH4$$

$$\frac{d\,NO3}{dt} = External + Internal + k_nitri \cdot NH4 - Uptake_NO3 - k_denitri \cdot NO3$$

Seaweed biomass changes through planting, growth, background mortality, sloughing, and harvest:

$$\frac{d\,Seaweed}{dt} = Planting + Seaweed_growth - M_rate \cdot Seaweed - S_rate(t) \cdot Seaweed - Harvest_40$$

Realized growth is limited by light, temperature, and nutrients:

$$Seaweed_growth = \mu \cdot F_I \cdot F_T \cdot F_N \cdot Seaweed$$

Limiter functions:

$$F_I = I \,/\, (K_I + I)$$

$$F_T = max(\,0, 1 - (T - T_opt)\text{^}2 \,/\, T_range\text{^}2\,)$$

$$F_N = max(\,F_NH4\,, F_NO3\,)$$

Substrate-specific nutrient limitation, with NH4 priority and inhibition on NO3 uptake:

$$F_NH4 = NH4 \,/\, (K_NH4 + NH4)$$

$$F_NO3 = [\,NO3 \,/\, (K_NO3 + NO3\,)\,] \cdot [\,1 \,/\, (\,1 + NH4 \,/\, K_I, inhib\,)\,]$$

Planting and harvest are represented as finite pulses over the 40-day cycle. Temperature, dissolved oxygen, and sloughing rate follow observed weekly schedules as time-varying forcings; numerical integration uses a daily step with Runge–Kutta.

Nitrogen demand and substrate partitioning:

$$N_required_for_growth = N_per_gram_biomass \cdot Seaweed_growth$$

$$Uptake_NH4 = Share_NH4 \cdot N_required_for_growth$$

$$Uptake_NO3 = (1 - Share_NH4) \cdot N_required_for_growth$$

Substrate share (piecewise):

$$Share_NH4 = F_NH4 \,/\, (F_NH4 + F_NO3) \quad if\ F_NH4 + F_NO3 > 0$$

$$Share_NH4 = 1\ otherwise$$

Table 1 compiles the model parameters (symbols, units, base values, roles) and indicates whether each term is fixed, calibrated, derived, or prescribed as a forcing; literature-based starts were refined during calibration.

Table 1. Input parameters and derived terms for the Takalar seaweed farm model, with SI units and parameter roles (fixed, calibrated, derived, forcing).

Symbol	Definition	Units	Value	Source/Notes	Role
NH4	Initial ammonium concentration	mg m^{-3}	1	Set from model start	Initial condition
NO3	Initial nitrate concentration	mg m^{-3}	20	Set from model start	Initial condition
μ_max	Maximum specific growth rate	d^{-1}	0.5	(11–13)	Calibrated
K_I	Half-saturation for light (FI)	arb. light units	50	Tuning	Fixed

Symbol	Definition	Units	Value	Source/Notes	Role
I	Incident light (constant in base run)	arb. light units	200	Tuning	Forcing
F_T	Temperature limitation function	dimensionless	—	FT = max(0, 1 − (T−Topt)^2/Trange^2)	Derived
T_opt	Optimal temperature	°C	28	(12)	Fixed
T_range	Thermal breadth parameter	°C	6	(12)	Fixed
F_NH4	NH_4^+ Monod term	dimensionless	—	NH4/(K_NH4+NH4)	Derived
F_NO3	NO_3^- Monod term with NH_4^+ inhibition	dimensionless	—	NO3/(K_NO3+NO3) · 1/(1+NH4/K_I_Inhibitor)	Derived
K_NH4	Half-saturation for NH_4^+ uptake	mg N m^{-3}	2	Model constant (Monod)	Fixed
K_NO3	Half-saturation for NO_3^- uptake	mg N m^{-3}	5	(4)	Fixed
K_I_Inhibitor	NH_4^+ inhibition constant on NO_3^- uptake	mg N m^{-3}	5	Tuning	Fixed
Share_NH4	Partition of N uptake to NH_4^+	dimensionless	—	F_NH4/(F_NH4+F_NO3)	Derived
N_per_gram_biomass	Nitrogen per gram of seaweed (WW)	mg N g^{-1} WW	3.57	(14)	Fixed
N_required_for_growth	Nitrogen demand supporting growth	mg N m^{-3} d^{-1}	—	N_per_gram_biomass × Seaweed_growth	Derived
kwnitri	Nitrification rate (water column)	d^{-1}	7	(15)	Fixed
kwdenitri	Denitrification rate (water column)	d^{-1}	0.05	Tuning	Fixed
kownitri	O_2 half-saturation for nitrification (if applied)	mg L^{-1}	1	(16)	Optional
Domestic_effluents	External nutrient input proxy	mg N m^{-3} d^{-1} (equiv.)	0.7	Represents domestic load	Forcing
River_runoff	Riverine nutrient input proxy	mg N m^{-3} d^{-1} (equiv.)	0	Represents river load (field observation)	Forcing
M_rate	Background natural mortality	d^{-1}	0.001	Biomass loss	Fixed
S_rate(t)	Time-varying sloughing rate	d^{-1}	0.02–0.04	Tuning	Forcing
H_rate	Harvest fraction at day 40	fraction	1	Full harvest pulse	Management
Seaweed_0	Initial planting density (per volume)	g WW m^{-3}	computed	From seed_per_tie, ties_per_m, line_length_m, lines_per_plot, plot_volume	Derived
seed_per_tie	Seed mass per tie	g WW tie^{-1}	22	Farm practice	Fixed
ties_per_m	Number of ties per meter	ties m^{-1}	5	Farm practice	Fixed
line_length_m	Line length per rope	m	1	Farm practice	Fixed
lines_per_plot	Number of lines in 10×15 m plot	—	10	Farm layout	Fixed
plot_volume	Active water volume over plot	m^3	15×10×0.5	Geometry × depth	Fixed
DO(t)	Dissolved oxygen schedule	mg L^{-1}	3.7–5.1	Field data	Forcing
T(t)	Temperature schedule	°C	29.7–30.8	Field data	Forcing

The numerical model was developed using STELLA Architect v1.6.0 (https://www.iseesystems.com). We ran the model for 40 days with a time step of 1/4. The calculations were performed using the fourth-order Runge–Kutta method. The outputs were compared with the values obtained from weekly field observations and the accuracy of validation was evaluated with the percent bias (PBIAS). PBIAS is a measure of over- and under-estimation of bias for predicted and measured values, and is expressed as a percentage (17). The performance rating in fitting of the model output to the observed value was evaluated with the following criteria [32]: very good (< ±25%), good (±25 PBIAS < ±40), satisfactory (±40 PBIAS < ±70), and non-satisfactory (≥ ±71).

3. Results and discussion

3.1 Example subsection heading

The calculated concentrations of ammonium (NH_4^+) and nitrate (NO_3^-) over the 40-day cultivation cycle are shown alongside observations in Fig. 2 (left and right panels, respectively).

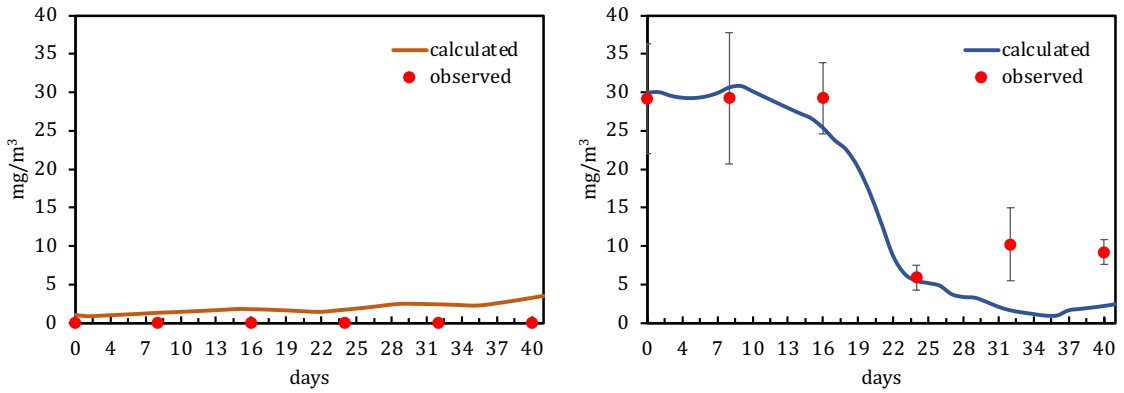


Figure 2. Dissolved inorganic nitrogen during the 40-day cultivation cycle. (a) Ammonium (NH_4^+) and (b) nitrate (NO_3^-) in the cultivation plot: colored lines are modelled concentrations (mg m^{-3}) and red points are weekly observations (mean; standard deviation bars)

Overall, the nitrate dynamics governed the nitrogen supply to the cultivation: concentrations started high, declined sharply mid-cycle, and partially recovered before harvest. In contrast, ammonium remained at or near the detection limit in the field samples throughout the cycle. The model reproduced the qualitative features of both nitrogen, low NH_4^+ and a pronounced mid-cycle NO_3^- decline, while revealing specific intervals of bias that help diagnose missing processes.

For ammonium, measured concentrations were effectively non-detectable across the cycle, consistent with rapid biological demand and efficient oxidation in these well-mixed nearshore waters. Ammonium is preferred by some seaweed species, including *Kappaphycus*, as it requires less energy for assimilation compared to nitrate, making it a more efficient nitrogen source for growth and metabolism (18,19). The model maintained NH_4^+ as a small but finite pool that rose slowly from ~1.0 to ~3.3 mg m^{-3} by Day 40. This gradual increase emerges from the balance between internal regeneration (sloughing and background mortality scaled to standing biomass) and removal via uptake and nitrification. This balance is influenced by various environmental factors, including temperature, nutrient availability, and microbial activity, which collectively regulate the rates of regeneration and removal processes in the ecosystem (20,21). Because field values were below detection, a percent-based bias metric is not tested; we therefore do not report PBIAS for NH_4^+ and instead evaluate the trajectory qualitatively. The small positive model values late in the cycle likely reflect an immediate routing of biomass losses to dissolved pools and a constant external input term (domestic effluents proxy) that does not diminish with time.

The nitrate time series presents a more distinct signal. Observed NO_3^- concentrations remained approximately 29–30 mg m^{-3} until Day 16, decreased to around 5.9 mg m^{-3} by Day 24, and subsequently increased to approximately 10.2 mg m^{-3} by Day 32 and 9.2 mg m^{-3} by Day 40. The model accurately captured the timing and magnitude of the decline, reaching approximately 5.5 mg m^{-3} by Day 24, but it underestimated the recovery in the later phase, maintaining levels around 2.0–2.2 mg m^{-3} near Days 39–40. Considering only the dates with observations (Days 0, 8, 16, 24, 32, and 40), the nitrate PBIAS was calculated to be −13.3%, indicating a slight overall

underestimation and categorizing it as very good (PBIAS < 25%). The negative bias is primarily attributed to the underestimation during the rebound phase.

Mechanistically, the model's behavior aligns with our process assumptions. In the initial phase, NO_3^- serves as the primary substrate for uptake, while NH_4^+ remains limited, facilitating rapid growth with minimal change in NH_4^+ levels. As biomass accumulates, internal regeneration increases NH_4^+ availability, and the model's uptake logic prioritizes NH_4^+ while inhibiting NO_3^- uptake through the Monod term. This, combined with denitrification, shifts the burden from NO_3^- and accelerates its mid-cycle reduction, replicating the observed trough. The late-cycle rebound observed in the data likely reflects episodic resupply, such as tidal exchange with adjacent waters, input from rainfall (not included in the model yet), wind-driven mixing, or minor riverine inputs, that is only broadly represented by the constant "external input" in the base configuration.

Two targeted refinements would plausibly reduce the residuals without over-fitting. First, adding a simple exchange term (or a two-box farm/open-water module) would allow NO_3^- to recover at observed rates after the minimum, avoiding the need to inflate background inputs. Second, routing a fraction of biomass losses into a short-lived organic-N pool that remineralizes with a delay would temper the small NH_4^+ rise late in the cycle while preserving internal recycling. If desired, DO-modulated nitrification/denitrification can be included to constrain transformations during low-oxygen episodes documented in the weekly DO forcing (22).

We note that the very good nitrate PBIAS (−13.3%) provides quantitative support for using this model to explore management scenarios. For ammonium, while no PBIAS is reported, the qualitative match—observed near-zero versus modeled small-but-non-zero—is acceptable given method limits and aligns with expectations for a system where rapid assimilation and nitrification keep NH_4^+ scarce. Together, these results suggest the model reproduces the first-order DIN dynamics relevant to growth and provides a defensible foundation for scenario testing and sensitivity analysis. For instance, the model could be employed to evaluate the system's response to varying nutrient input levels under different environmental conditions like other studies (23,24).

Observed seaweed biomass (g m^{-3}) increased throughout the 40-day cycle but with distinct phases. A rapid early rise was recorded from 23.18 (Day 0) to 44.41 (Day 8) and 66.47 (Day 16). Growth then slowed markedly around the middle of the cycle, with biomass near 69.41 (Day 24) and 74.24 (Day 32). A late-cycle recovery followed, reaching 105.29 by harvest (Day 40). This three-stage profile: fast increase, mid-cycle shoulder, modest end-phase gain, is consistent with transient nutrient limitation punctuating otherwise favorable conditions.

The model reproduced the overall trajectory and inflection points but showed phase-dependent bias. It underestimated biomass during the early–mid phase (e.g., Day 8: 31.54 vs 44.41; Day 16: 49.57 vs 66.47 g m^{-3}), tracked observations closely near the mid-cycle shoulder (Day 24: 73.44 vs 69.41 g m^{-3}), and overestimated late in the cycle (Day 32: 100.19 vs 74.24; Day 40: 135.05 vs 105.29 g m^{-3})(Figure 3.). Despite these shifts, the model captured the dominant features of the growth curve that matter for production planning.

Reproducibility evaluated with percent bias (PBIAS) over the six observed dates (Days 0, 8, 16, 24, 32, 40) was +8.1%, which falls in the very good category (PBIAS < 25%). The positive sign indicates a small overall overestimation, driven primarily by the late-cycle points. In other words, the model slightly overshoots harvest-time biomass while remaining close to observations at the mid-cycle shoulder and only modestly low during the earliest interval.

The biomass pattern aligns closely with the nitrogen sequence described earlier. The fast early growth coincides with high NO_3^- (~30 mg m^{-3}), the mid-cycle slowdown with the NO_3^- minimum (~6 mg m^{-3} around Day 24), and the late-cycle recovery with the partial rebound of NO_3^-. This DIN–growth coupling is also expressed in the model's limiter structure: as nitrate declines, limiter drops and growth slows; when nitrate recovers, limiter rises and growth resumes.

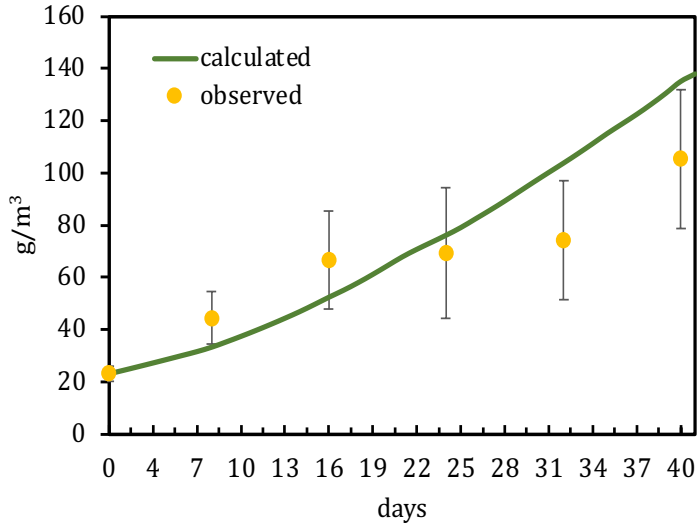


Figure 3. Time series of *Kappaphycus alvarezii* biomass during a 40-day cultivation cycle in Takalar, South Sulawesi. The green line shows modelled biomass (g m^{-3}); yellow points are observed weekly means from the farm plot (n = 17 thalli per week), with standard deviation bars.

The model's late-phase overestimation is plausibly linked to internal recycling and substrate preference. As standing biomass accumulates, sloughing and natural mortality regenerate NH_4^+. Given NH_4^+ priority and inhibition of NO_3^- uptake in the formulation, even a modest NH_4^+ supply can keep limiter value relatively elevated after the nitrate trough, sustaining modeled growth more than observed. In the field, the end-phase increase was more muted, suggesting non-nutrient constraints (e.g., epiphytes, diseases, or slightly higher effective loss rates) that are only partially represented by the current sloughing and mortality terms (25–27).

Taken together, the trend agreement and very good PBIAS indicate that the model captures the first-order controls of DIN variability on biomass accumulation across the cultivation cycle. For management, this means the system is most responsive early—when nitrate is abundant—and most vulnerable mid-cycle, when nitrate dips. Monitoring NO_3^- around Days 20–30, staggering planting to spread peak nitrogen demand, and modestly increasing late-phase loss terms (or introducing a short-lived organic-N pool) are supported by the diagnostics and would likely reduce the end-phase bias without degrading performance earlier in the cycle.

The model effectively demonstrates the growth of nitrogen and seaweed throughout the farming cycle. To enhance its accuracy, incorporating factors such as tides, rain, and wind could improve predictions of nitrate levels at the cycle's conclusion. Implementing a dual system for farm and open water, along with a short-term organic nitrogen pool, might enhance the model's representation of nutrient cycling and biomass growth. In essence, the 40-day data indicates that nitrate is crucial for farm production: early nitrate availability promotes rapid growth, a mid-cycle

decline slows growth, and some nitrate reappears before harvest, while ammonium remains a minor, rapidly fluctuating component. The model aligns well with these patterns (nitrate PBIAS −13.3%, biomass PBIAS +8.1%), providing a solid foundation for management and testing. The bias checks suggest practical model improvements by incorporating water exchange with open water and including other nitrogen-utilizing competitors, such as phytoplankton and epiphytes.

4. Conclusion

Integrating weekly field measurements with a mass balanced system dynamics model shows that dissolved inorganic nitrogen variability, especially nitrate, is a first order control on *Kappaphycus alvarezii* biomass accumulation across a single 40 day cultivation cycle in Takalar. The model reproduces the key system behavior observed in the field: ammonium remains effectively scarce in the water column, while nitrate exhibits a pronounced mid cycle drawdown that coincides with a clear growth slowdown, followed by partial recovery before harvest. Model performance was very good for both nitrate (PBIAS −13.3%) and biomass (PBIAS +8.1%), indicating that the model captures the dominant dynamics at the cultivation cycle scale, and the remaining mismatches point to specific processes that should be improved in future model versions. In particular, the underestimated late cycle nitrate rebound and the tendency to over predict late biomass suggest that exchange and additional loss or competition processes are not yet fully represented, rather than indicating a weakness in the core nitrogen growth linkage. Overall, the validated framework can be used for further scenario analysis and sensitivity testing. This establishes a cycle scale tool for diagnosing nitrogen limitation and quantifying its implications for harvestable biomass under the observed conditions.

Acknowledgment

The authors gratefully acknowledge Hasanuddin University for financial support through the PDPU Research Grant for Fiscal Year 2025 under Contract No. 01260/UN4.22/PT.01.03/2025. The authors also sincerely thank the anonymous reviewers for their valuable comments and constructive suggestions, which helped improve the quality of this manuscript.

References

[1] He Q and Silliman BR 2019 Climate change, human impacts, and coastal ecosystems in the Anthropocene *Curr. Biol.* 29 R1021-R1035 (doi:10.1016/j.cub.2019.08.042)
[2] Voss M, Bange HW, Dippner JW, Middelburg JJ, Montoya JP and Ward B 2013 The marine nitrogen cycle: recent discoveries, uncertainties and the potential relevance of climate change *Philos. Trans. R. Soc. B Biol. Sci.* 368 20130121 (doi:10.1098/rstb.2013.0121)
[3] Diaz RJ and Rosenberg R 2008 Spreading dead zones and consequences for marine ecosystems *Science* 321 926-929 (doi:10.1126/science.1156401)
[4] Narvarte BCV, Genovia TGT, Hinaloc LAR and Roleda MY 2022 Growth, nitrate uptake kinetics, and biofiltration potential of eucheumatoids with different thallus morphologies *J. Phycol.* 58 12-21 (doi:10.1111/jpy.13229)
[5] Rimmer MA, Sugama K, Rakhmawati D, Rofiq R and Habgood RH 2013 A review and SWOT analysis of aquaculture development in Indonesia *Rev. Aquac.* 5 255-279 (doi:10.1111/raq.12017)
[6] Roleda MY and Hurd CL 2019 Seaweed nutrient physiology: application of concepts to aquaculture and bioremediation *Phycologia* 58 552-562 (doi:10.1080/00318884.2019.1622920)

[7] Sarri JH, Abdulmutalib YA, Mohammad Tilka ME, Terzi E and Tahiluddin AB 2022 Effects of inorganic nutrient enrichment on the carrageenan yield, growth, and ice-ice disease occurrence of red alga *Kappaphycus striatus Aquat. Res.* 5 99-109 (doi:10.3153/ar22009)
[8] Tahiluddin AB, Nuñal SN and Santander-de Leon SMS 2022 Inorganic nutrient enrichment of seaweed *Kappaphycus*: farmers' practices and effects on growth and ice-ice disease occurrence *Reg. Stud. Mar. Sci.* 55 102593 (doi:10.1016/j.rsma.2022.102593)
[9] Alam JF, Yamamoto T, Umino T, Nakahara S and Hiraoka K 2020 Estimating nitrogen and phosphorus cycles in a timber reef deployment area *Water* 12 2515 (doi:10.3390/w12092515)
[10] Muralidhar M, Kumar JA, Suvana S, Jayanthi M, Vishwajeet P and Dayal JS 2024 Dynamic modelling of coastal aquaculture systems: a review *Aquat. Ecosyst. Health Manag.* 26 40-52 (doi:10.14321/aehm.026.03.40)
[11] Ohno M, Largo DB and Ikumoto T 1994 Growth rate, carrageenan yield and gel properties of cultured kappa-carrageenan producing red alga *Kappaphycus alvarezzi* (Doty) Doty in the subtropical waters of Shikoku, Japan *J. Appl. Phycol.* 6 1-5 (doi:10.1007/BF02185896)
[12] Kumar YN, Poong SW, Gachon C, Brodie J, Sade A and Lim PE 2020 Impact of elevated temperature on the physiological and biochemical responses of *Kappaphycus alvarezii* (Rhodophyta) *PLoS One* 15 e0239097
[13] Aslan LOM, Cahyani H, Hardianti H, Kurnia DP, Febriani A, Prity NA, Ariskanti, Anastasia H, Dinaswati and Iba W 2020 Field cultivation of *Kappaphycus alvarezii* (Doty) Doty ex Silva using tissue-cultured seedlings at Bungin Permai coastal waters, South Konawe, Southeast Sulawesi: the third year of seaweed growth monitoring *IOP Conf. Ser. Earth Environ. Sci.* 473 012007 (doi:10.1088/1755-1315/473/1/012007)
[14] Angell AR, Mata L, de Nys R and Paul NA 2016 The protein content of seaweeds: a universal nitrogen-to-protein conversion factor of five *J. Appl. Phycol.* 28 511-524 (doi:10.1007/s10811-015-0650-1)
[15] Chen S, Ling J and Blancheton JP 2006 Nitrification kinetics of biofilm as affected by water quality factors *Aquac. Eng.* 34 179-197 (doi:10.1016/j.aquaeng.2005.09.004)
[16] Chapelle A, Ménesguen A, Deslous-Paoli JM, Souchu P, Mazouni N, Vaquer A and Millet B 2000 Modelling nitrogen, primary production and oxygen in a Mediterranean lagoon: impact of oysters farming and inputs from the watershed *Ecol. Modell.* 127 161-181 (doi:10.1016/S0304-3800(99)00206-9)
[17] Gupta HV, Sorooshian S and Yapo PO 1999 Status of automatic calibration for hydrologic models: comparison with multilevel expert calibration *J. Hydrol. Eng.* 4 135-143 (doi:10.1061/(ASCE)1084-0699(1999)4:2(135))
[18] Dy DT and Yap HT 2001 Surge ammonium uptake of the cultured seaweed *Kappaphycus alvarezii* (Doty) Doty (Rhodophyta: Gigartinales) *J. Exp. Mar. Biol. Ecol.* 265 89-100 (doi:10.1016/S0022-0981(01)00325-2)
[19] Husna Zuldin W and Shapawi R 2015 Performance of red seaweed (*Kappaphycus* sp.) cultivated using tank culture system *J. Fish. Aquat. Sci.* 10 1-12 (doi:10.3923/jfas.2015.1.12)
[20] Lin X, Li X, Gao D, Liu M and Cheng L 2017 Ammonium production and removal in the sediments of Shanghai river networks: spatiotemporal variations, controlling factors, and environmental implications *J. Geophys. Res. Biogeosci.* 122 2461-2478 (doi:10.1002/2017JG003769)
[21] Kim KY 2024 Harnessing seaweed farming for climate mitigation in South Korea: evaluating carbon dioxide removal potential and future research directions *Algae* 39 329-347 (doi:10.4490/algae.2024.39.10.28)
[22] Daigger GT, Adams CD and Steller HK 2007 Diffusion of oxygen through activated sludge flocs: experimental measurement, modeling, and implications for simultaneous nitrification and denitrification *Water Environ. Res.* 79 375-387 (doi:10.2175/106143006X111835)
[23] Nev OA, Lindsay RJ, Jepson A, Butt L, Beardmore RE and Gudelj I 2021 Predicting microbial growth dynamics in response to nutrient availability *PLoS Comput. Biol.* 17 e1008817 (doi:10.1371/journal.pcbi.1008817)
[24] Piroddi C *et al* 2021 Effects of nutrient management scenarios on marine food webs: a pan-European assessment in support of the Marine Strategy Framework Directive *Front. Mar. Sci.* 8 596797 (doi:10.3389/fmars.2021.596797)
[25] Worm B and Sommer U 2000 Rapid direct and indirect effects of a single nutrient pulse in a seaweed-epiphyte-grazer system *Mar. Ecol. Prog. Ser.* 202 283-288 (doi:10.3354/meps202283)

[26] Porada P and Giordani P 2021 Bark water storage plays key role for growth of Mediterranean epiphytic lichens *Front. For. Glob. Change* 4 668682 (doi:10.3389/ffgc.2021.668682)
[27] Ward GM, Kambey CSB, Faisan JP, Tan PL, Daumich CC, Matoju I, Stentiford GD, Bass D, Lim PE, Brodie J and Poong SW 2022 Ice-ice disease: an environmentally and microbiologically driven syndrome in tropical seaweed aquaculture *Rev. Aquac.* 14 414-439 (doi:10.1111/raq.12606)